

Optimal control of acute myeloid leukaemia

Jesse A Sharp^{1,2} Alexander P Browning^{1,2} Tarunendu Mapder^{1,2}
Kevin Burrage^{1,2,3} *Matthew J Simpson¹

¹ *School of Mathematical Sciences, Queensland University of Technology (QUT)
Australia.*

² *ARC Centre of Excellence for Mathematical and Statistical Frontiers, QUT,
Australia.*

³ *Department of Computer Science, University of Oxford, UK (Visiting
Professor).*

Abstract

Acute myeloid leukaemia (AML) is a blood cancer affecting the haematopoietic stem cells of the myeloid cell line. AML is routinely treated with chemotherapy, and so it is of great interest to develop optimal chemotherapy treatment strategies. In this work, we incorporate an immune response into a stem cell model of AML, since we find that previous models lacking an immune response are inappropriate for deriving optimal control strategies. Using optimal control theory, we produce continuous controls and bang-bang controls, corresponding to a range of objectives and parameter choices. Through example calculations, we provide a practical approach to applying optimal control using Pontryagin's maximum principle. In particular, we describe and explore factors that have a profound influence on numerical convergence. We find that the convergence behaviour is sensitive to the method of control updating, the nature of the control, and to the relative weighting of terms in the objective function. All codes we use to implement optimal control are made available.

Key words: Leukaemia; Stem cells; Immune response; Optimal treatment.

1 Introduction

2 Acute Myeloid Leukaemia (AML) is a blood cancer that is characterised by
3 haematopoietic stem cells of the myeloid cell line, primarily in the bone mar-
4 row, transforming into leukaemic blast cells [21,46]. These blast cells no longer
5 undergo normal differentiation or maturation and stop responding to normal
6 regulators of proliferation [22]; their presence in the bone marrow niche dis-
7 rupts normal haematopoiesis [21]. AML has significant mortality rates, with
8 a five-year survival rate of 24.5% [7], and challenges in treatment arise not
9 only in eradication of the leukaemic cells but also prophylaxis and treatment
10 of numerous life threatening complications that arise due to the absence of
11 sufficient healthy blood cells [61]. Multiple interventions are employed in the
12 management and treatment of AML, including: leukapheresis; haematopoi-
13 etic stem cell transplants; radiotherapy; chemotherapy and immunotherapy
14 [4,46,51].

15 Mathematical models are widely used to gain insight into complex biologi-
16 cal processes [28,47]. Mathematical models facilitate the development of novel
17 hypotheses, allow us to test assumptions, improve our understanding of bio-
18 logical interactions, interpret experimental data and assist in the generating
19 parameter estimates. Furthermore, mathematical models provide a convenient,
20 low-cost mechanism for investigating biological processes and interventions for
21 which experimental data may be scarce, cost-prohibitive or difficult to obtain
22 owing to ethical issues. Mathematical models are routinely used to interro-
23 gate a variety of processes relating to cancer research including; incidence;
24 development and metastasis; tumour growth; immune reaction and treatment
25 [12,15,21,30,42,58]. Recently, mathematical models have been used to inves-
26 tigate various aspects of AML, including: incidence [40]; pathogenesis [18];

* Corresponding author

Email address: matthew.simpson@qut.edu.au, *Telephone* + 61 7 31385241,
Fax + 61 7 3138 2310 (*Matthew J Simpson¹).

27 interactions between cancer and healthy haematopoietic stem cells within the
28 bone marrow niche [21]; and recurrence following remission [49].

29 Determining how to apply optimally a treatment such as chemotherapy is of
30 great practical and theoretical interest. Chemotherapy, a common treatment
31 for AML [20], is associated with significant health costs related to the cyto-
32 toxicity of chemotherapeutic agents [10,46], but also substantial economic cost
33 [63]. Optimal control theory provides us with tools for determining the optimal
34 way to apply a control to a model such that some desired quantities of interest
35 are minimised or maximised. Optimal control has been applied to a range of
36 medically motivated biological models recently; including vaccination, tumour
37 therapy and drug scheduling [14,16,34,35,43].

38 In this work we consider a recent haematopoietic stem cell model of AML
39 [21]. After examining the steady state behaviour associated with this model,
40 we make a biologically appropriate and mathematically convenient modifica-
41 tion by incorporating an immune response in the form of a Michaelis-Menten
42 kinetic function. Overall, in this work we pursue two broad aims:

- 43 (1) Determine how to apply optimal control to the model, accounting for key
44 clinical features such as the competition between the negative effects of
45 the disease and the negative effects of the treatment;
- 46 (2) Provide a concise and insightful discussion of the methodology and nu-
47 merical implementation of optimal control, as we find that much of the
48 existing literature is opaque with regard to practical implementation.

49 In addressing these aims, we provide a brief introduction to the theory of
50 optimal control and apply optimal control techniques to the modified model,
51 identifying optimal treatment strategies under a variety of circumstances. This
52 leads us to consider both continuous and discontinuous bang-bang optimal
53 controls. Our work provides a comprehensive discussion of practical issues
54 that can arise when applying optimal control, and we explore key factors

55 that influence numerical convergence when using a forward-backward sweep
56 algorithm to solve two-point boundary value problems that arise. The codes we
57 use to implement the algorithms associated with the optimal control solutions
58 is freely available on GitHub.

59 In Section 2 we present a haematopoietic stem cell model of AML [21], and
60 discuss the steady states. In Section 3 the importance of an immune response
61 is outlined, and the model is modified to include such a response. In Section
62 4, we present discussion and results of optimal control applied to the modified
63 AML model. Finally, concluding remarks are provided in Section 5

64 **2 Acute myeloid leukaemia model**

65 Crowell, MacLean and Stumpf [21] propose a system of ordinary differential
66 equations (ODEs) to model AML. Their model can be written as,

$$\begin{aligned}\frac{dS}{dt} &= \rho_s S(K_1 - Z_1) - \delta_S S, \\ \frac{dA}{dt} &= \delta_S S + \rho_A A(K_2 - Z_2) - \delta_A A, \\ \frac{dD}{dt} &= \delta_A A - \mu_D D, \\ \frac{dL}{dt} &= \rho_L L(K_2 - Z_2) - \delta_L L, \\ \frac{dT}{dt} &= \delta_L L - \mu_T T.\end{aligned}\tag{1}$$

67 Here $S(t)$, $A(t)$, $D(t)$, $L(t)$ and $T(t)$ represent haematopoietic stem cells, pro-
68 genitor cells, terminally differentiated cells of $S(t)$, leukaemia stem cells and
69 fully differentiated leukaemia cells, respectively. $Z_1(t) = S(t)$ and $Z_2(t) =$
70 $A(t) + L(t)$, where $A(t)$ and $L(t)$ are coupled as the proliferating leukaemia
71 population ($L(t)$) competes with the haematopoietic progenitor cell popu-

72 lation ($A(t)$). This competition is motivated in [21] by the hypothesis that
73 leukaemic stem cells and haematopoietic stem cells occupy the same niche
74 within the bone marrow [25,57] and hence compete for resources. This niche
75 interaction has been demonstrated as being crucial to similar haematopoietic
76 and leukaemic cell models of chronic myeloid leukaemia [42]. Throughout this
77 work we present numerical solutions to this model and other related mod-
78 els. In all solutions presented the parameters are dimensionless, such that the
79 time scale is arbitrary and cell population sizes within the bone marrow are
80 expressed as a portion of the carrying capacities, such that $K_1 = K_2 = 1$. Set-
81 ting these carrying capacities to be of equal size is a simplifying assumption
82 in our analysis, though we note that this is not required, and could be relaxed
83 if suitable alternative estimates of the carrying capacities were identified.

84 Crowell, MacLean and Stumpf use numerical solutions of Equation (1) to iden-
85 tify parameter values that lead to particular long time steady state solutions
86 of the model. In this work we will use standard variables to denote time de-
87 pendent quantities, such as $S(t)$, and an overbar to denote long-time steady
88 quantities, such as $\lim_{t \rightarrow \infty} S(t) = \bar{S}$. The parameters we use are summarised in
89 Table 1, and we note that the model supports three non-trivial steady states:

- 90 (1) The *healthy* steady state consists of $\bar{S}, \bar{A}, \bar{D} > 0$ and $\bar{L} = \bar{T} = 0$, such
91 that there is a population of each healthy cell species and no leukaemia
92 is present.
- 93 (2) The *coexisting* steady state requires $\bar{S}, \bar{A}, \bar{D}, \bar{L}, \bar{T} > 0$ simultaneously. In
94 this work we are interested in modelling the optimal application of an
95 intervention (or control) such as chemotherapy to the system that shifts
96 it from the coexisting steady state towards the healthy steady state.
- 97 (3) The third steady state is *leukaemic*, characterised by $\bar{S} = \bar{A} = \bar{D} = 0$
98 and $\bar{L}, \bar{T} > 0$, such that only leukaemic cells are present.

99 The leukaemic steady state is less interesting from an intervention perspective

100 as it cannot be steered towards the healthy steady state via a control such as
101 chemotherapy alone; requiring in addition a source of healthy cells.

Table 1: Parameters values used in this work.

Parameter description	Value
Proliferation of S	$\rho_S = 0.5$
Proliferation of A	$\rho_A = 0.43$
Proliferation of L	$\rho_L = 0.27$
Differentiation of S into A	$\delta_S = 0.14$
102 Differentiation of A into D	$\delta_A = 0.44$
Differentiation of L into T	$\delta_L = 0.05$
Migration of D into the blood stream	$\mu_D = 0.275$
Migration of T into the blood stream	$\mu_T = 0.3$
Carrying capacity of the compartment with S	$K_1 = 1$
Carrying capacity of the compartment with A and L	$K_2 = 1$
Characteristic rate of the immune response	$\alpha = 0.015$
Half saturation constant of the immune response	$\gamma = 0.01$

103 Parameter values in Table 1 are used in all numerical solutions presented in this
104 work, unless otherwise indicated. These values match those specified in [21]
105 to produce a healthy steady state, noting that [21] included parameter sweeps
106 over ρ_S, ρ_A, δ_S and δ_A , with the exception of δ_L . We have set $\delta_L = 0.05$ to
107 produce the coexisting steady state, although other values for δ_L also produce
108 this coexisting steady state.

109 Schematics showing the key features of the original model, a modified model
110 that incorporates an immune response (Section 3), and the modified model
111 subject to a control (Section 4) are presented in Figure 1. Typical numerical
112 solutions of the original model are presented in Figure 2. All numerical results
113 presented in this study are obtained using a fourth-order Runge-Kutta method
114 [52] with a constant time step of $\delta t = 0.001$. We find that this choice is

115 sufficient to produce numerical solutions that are grid-independent. From the
116 numerical results we observe that for the parameter values given in Table 1,
117 provided that initially $S(0) > 0$ and $L(0) > 0$, the system will tend towards
118 the coexisting steady state. In Section 3 we modify the model to incorporate
119 an immune response, such that sufficiently small leukaemic populations will
120 decay without intervention.

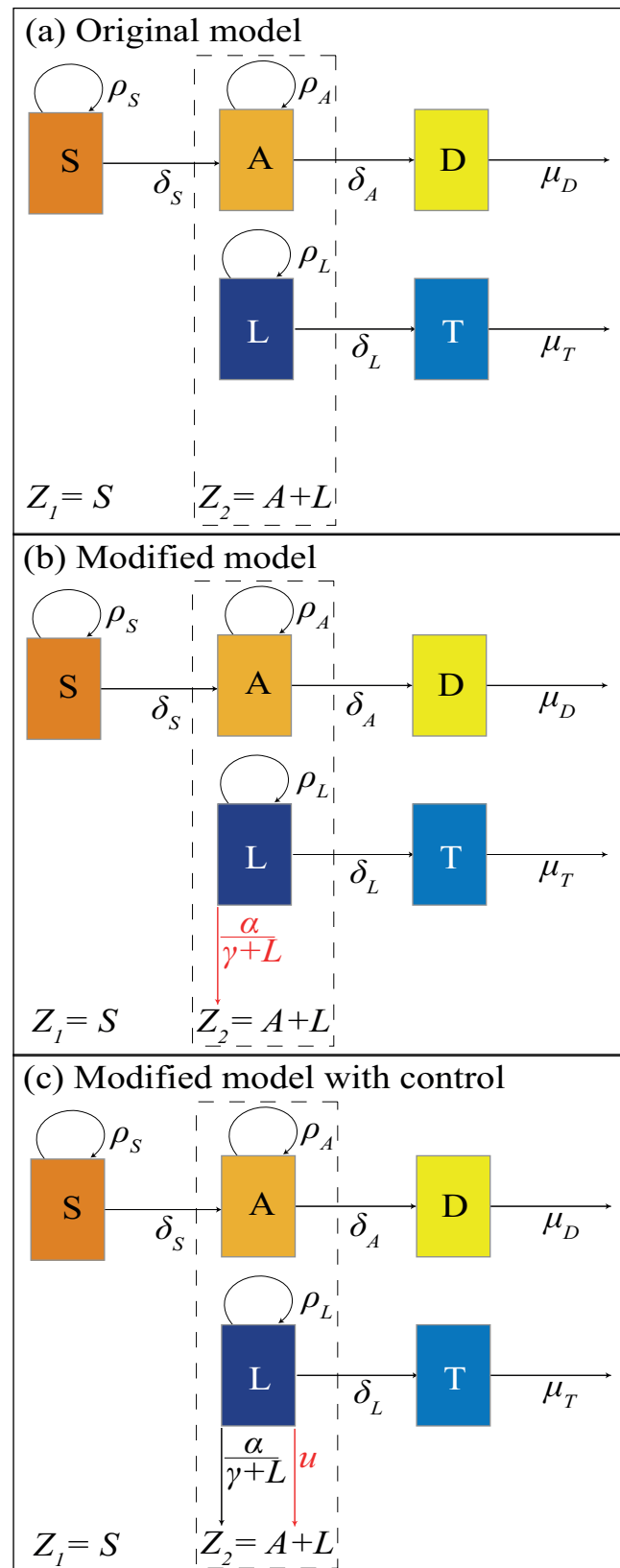


Fig. 1. Schematics present the interactions and associated parameters for the (a) original model [21], (b) modified model with immune response and (c) modified model subject to a control, u . In each schematic the additional response is highlighted in red.

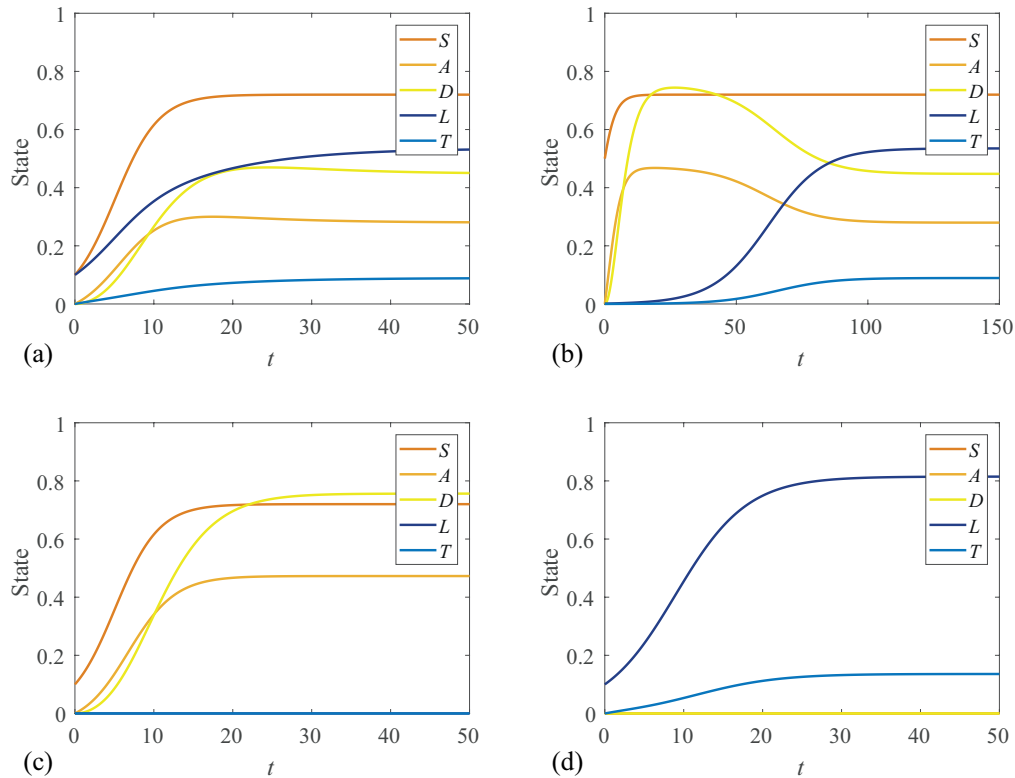


Fig. 2. Numerical solutions of Equations 1 for various initial conditions: (a) Coexisting steady state solution with $[S(0), A(0), D(0), L(0), T(0)] = [0.1, 0, 0, 0.1, 0]$. (b) Coexisting steady state with $[0.5, 0, 0, 10^{-3}, 0]$. (c) Healthy steady state with $[0.1, 0, 0, 0, 0]$. (d) Leukaemic steady state with $[0, 0, 0, 0.1, 0]$.

121 In Figure 2b we note that although the initial leukaemia stem cell population is
 122 small compared to the initial haematopoietic stem cell population, the system
 123 eventually evolves to the same coexisting steady state as in Figure 2a. However,
 124 this steady state condition requires a longer timescale to develop from the
 125 different initial conditions.

126 3 Incorporating the immune response

127 The immune system is known to play a critical role in the development, metas-
 128 tasis, treatment and recurrence of cancers [24,26]. This knowledge is supported
 129 by a range of clinical evidence, including a well-documented increased risk
 130 of cancer incidence in patients with immunodeficiency [17]. This is exempli-

131 fied by experimental mouse models where mice are typically immunocompro-
132 mised to avoid transplanted cancers being destroyed by the immune response
133 in xenograft studies [19]. Furthermore, tumours found in immunocompetent
134 hosts are observed to exhibit mechanisms for avoiding immune response [45].

135 The behaviour exhibited in Figure 2b indicates that the system cannot reach
136 a healthy non-leukaemic steady state in the presence of even small leukaemic
137 stem cell populations. It is reasonable to expect that under some circum-
138 stances a small leukaemic population may be outcompeted by healthy cells
139 occupying the same niche [41], without intervention. Therefore, we consider a
140 modification to the model proposed by Crowell, MacLean and Stumpf to incor-
141 porate an immune response. We expect this immune response to be effective
142 for small L and ineffective for large L , and so we mimic this by introducing a
143 Michaelis-Menten term to represent the immune response, giving,

$$\begin{aligned}\frac{dS}{dt} &= \rho_s S(K_1 - Z_1) - \delta_S S, \\ \frac{dA}{dt} &= \delta_S S + \rho_A A(K_2 - Z_2) - \delta_A A, \\ \frac{dD}{dt} &= \delta_A A - \mu_D D, \\ \frac{dL}{dt} &= \rho_L L(K_2 - Z_2) - \delta_L L - \underbrace{\frac{\alpha L}{\gamma + L}}_{\text{immune response}}, \\ \frac{dT}{dt} &= \delta_L L - \mu_T T.\end{aligned}\tag{2}$$

144 Including an immune response in the model is not only mathematically con-
145 venient in that it provides desirable steady states that we discuss later in this
146 section, but also biologically relevant. Immune responses are widely studied
147 in both the theoretical and experimental biology literature and acknowledged
148 as an important contributor to pathogenesis and tumour dynamics in AML
149 [6,31,60]. Additionally, immunotherapy is being investigated as an alternative
150 to chemotherapy for treatment of AML and many other cancers [9,39,44].

151 Michaelis-Menten terms are commonly used to incorporate immune responses
 152 in other biologically motivated models [2,23,37]. However, it is unclear, simply
 153 by inspection, what parameter values are required to obtain two stable steady
 154 states: one coexisting and one healthy. For $\gamma \ll \alpha$ the Michaelis-Menten term
 155 behaves as exponential decay at a rate of α , while for $\gamma \gg L$ it behaves as a
 156 linear sink term [55,56]. Intuitively, we expect setting $\gamma = \mathcal{O}(L)$ will produce
 157 the desired dynamics whereby the immune response is effective for small L
 158 and ineffective for large L .

159 We investigate further by considering the potential steady states permitted
 160 by Equation (2). We note that S is governed by a logistic growth mechanism
 161 that does not depend on any of the other species so we have $\bar{S} = 1 - \delta_S/\rho_S$.
 162 Similarly, D and T do not influence the other populations and hence can be
 163 neglected in the consideration of the steady states. Therefore, we consider a
 164 reduced system in terms of A, L with $\bar{S} = 1 - \delta_S/\rho_S$, recalling that $Z_2 = A + L$,
 165 and through scaling $K_2 = 1$,

$$\frac{dA}{dt} = f(A, L) = \delta_S \left(1 - \frac{\delta_S}{\rho_S} \right) + \rho_A A(1 - A - L) - \delta_A A, \quad (3)$$

$$\frac{dL}{dt} = g(A, L) = \rho_L L(1 - A - L) - \delta_L L - \frac{\alpha L}{\gamma + L}. \quad (4)$$

166 By inspection, there is a trivial L-nullcline at $\bar{L} = 0$. We can find the A-
 167 nullcline by setting $f(A, L) = 0$ in Equation (3),

$$\bar{L} = \frac{\delta_S \bar{S}}{\rho_A A} + 1 - A - \frac{\delta_A}{\rho_A}. \quad (5)$$

168 Similarly, we can find the non-trivial L-nullcline by setting $g(A, L) = 0$ in
 169 Equation (4),

$$\bar{A} = 1 - L - \frac{\delta_L}{\rho_L} - \frac{\alpha}{\rho_L(\gamma + L)}. \quad (6)$$

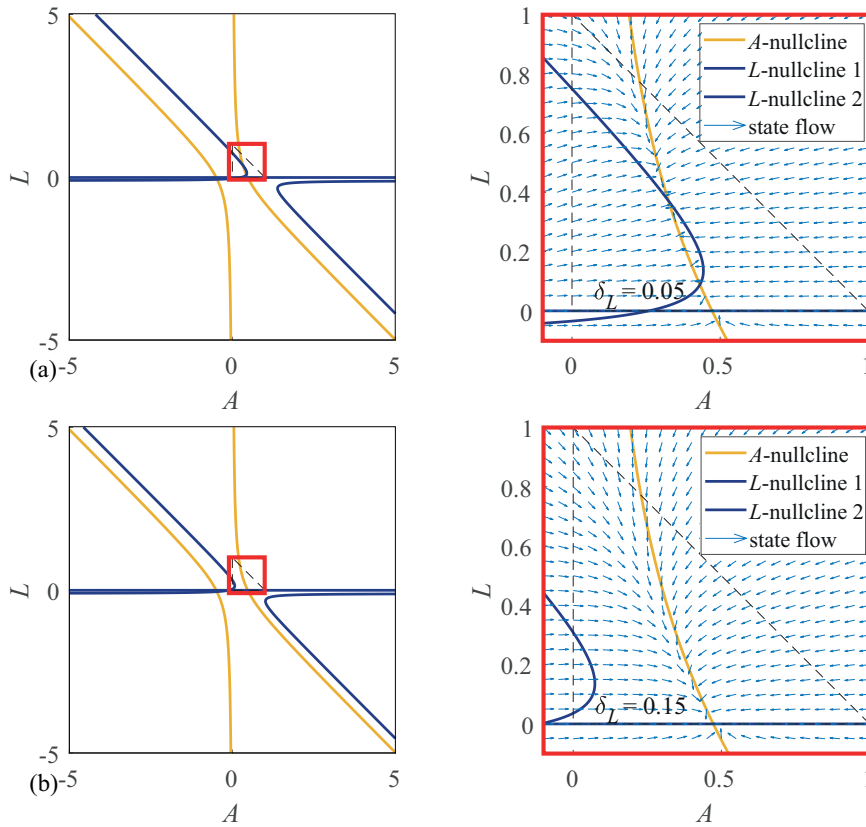


Fig. 3. Nullclines using parameters for (a) a coexistence steady state; $[\rho_S, \rho_A, \rho_L, \delta_S, \delta_A, \delta_L] = [0.5, 0.43, .027, 0.14, 0.44, 0.05]$, and (b) the same parameters with application of a control of $u \equiv 0.1$, effectively increasing δ_L to 0.15 (a control could be a treatment such as chemotherapy that increases the rate of decay of leukaemic stem cells, this is discussed in Section 4). In (a), for particular choices of the introduced parameters α and γ it is possible for the hyperbolas to intersect twice within the physically realistic region (dashed triangle). These figures are produced with $\alpha = 0.015$, $\gamma = 0.1$.

170 The nullclines, given by Equations (5) and (6), are hyperbolas. In Figure 3
 171 we present phase planes showing dynamics of the A and L populations within
 172 the physically meaningful region, $A + L \leq 1$.

173 This system has the desired property that we outlined previously, namely
174 that there is a stable steady state of coexistence that we aim to steer to the
175 stable state with no leukaemia through applying optimal control. Numerical
176 solutions of the modified model with no control are presented in Figure 4.

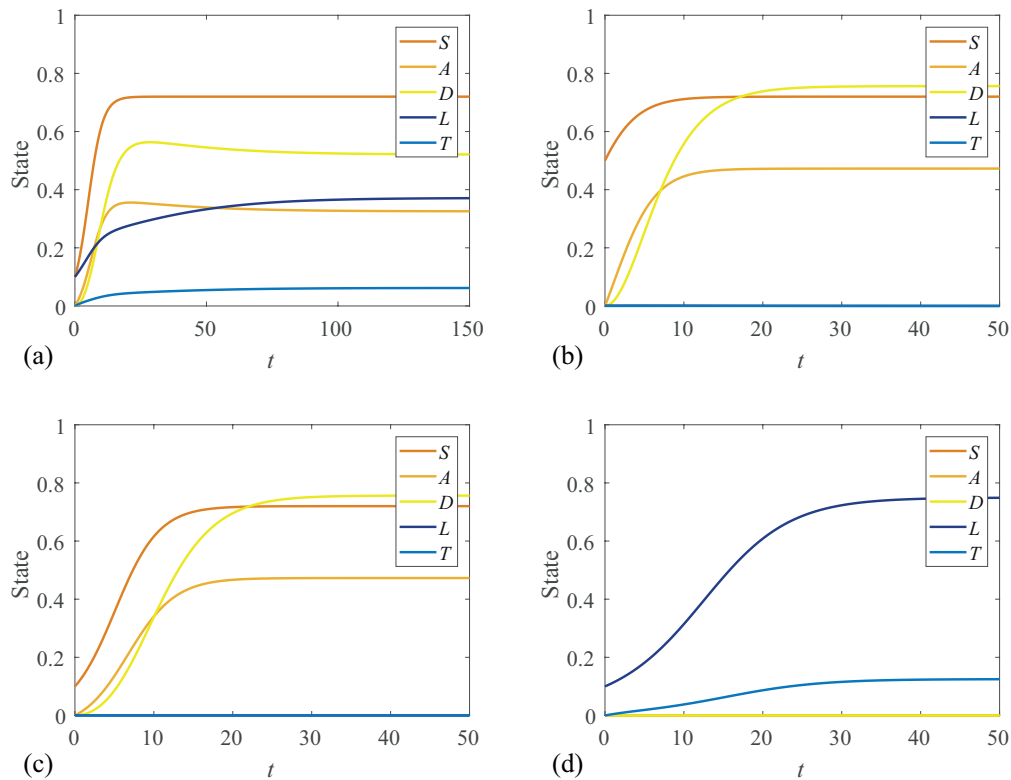


Fig. 4. Numerical solutions to the modified model with an immune response for initial conditions corresponding to Figure 2. In (a) we observe coexistence, though it takes longer for the solutions to approach steady state when compared with the original model (Figure 2a). This result is presented over a larger time-scale. With the introduction of the Michaelis-Menten style immune response to leukaemia, we observe in (b) that a small leukaemia stem cell population does not survive in the presence of a haematopoietic stem cell population. This is in contrast to Figure 2b, where a minute population of leukaemic stem cells was sufficient to grow to a coexisting steady state. These figures are produced with immune response parameters $\alpha = 0.015$, $\gamma = 0.1$.

177 4 Results and discussion

178 In this section we provide a concise overview of the theory of optimal control.
179 Methods for solving optimal control problems are discussed. We determine
180 optimal controls to the model presented in Section 3. Specifically, we consider
181 continuous optimal controls corresponding to quadratic pay-off functions and
182 discontinuous bang-bang optimal controls corresponding to linear pay-off func-
183 tions. Numerical solutions are produced for several different pay-off weighting
184 parameter combinations.

185 4.1 Optimal control theory

186 The basic principle of optimal control is to apply an external force, the *control*,
187 to a system of differential equations, the *state equations*, to cause the solution,
188 the *state*, to follow a new trajectory and/or arrive at a different final state.
189 The goal of optimal control is to select a particular control that maximises or
190 minimises a chosen objective functional, the *pay-off*; typically a function of the
191 state and the control. The pay-off is chosen such that the new trajectory/final
192 state are preferred to that of the uncontrolled state, accounting for any cost
193 associated with applying the control.

194 A typical optimal control problem will introduce the state equations as func-
195 tions of the state $\mathbf{x}(t)$ and the control $u(t)$, with initial state $\mathbf{x}(0) = \mathbf{x}_0$,

$$\frac{d\mathbf{x}}{dt} = f(t, \mathbf{x}(t), u(t)), \quad \mathbf{x}(t) \in \mathbb{R}^n. \quad (7)$$

196 It is also necessary to specify either a final time t_f with the final state free, or
197 a final state $\mathbf{x}(t_f)$, with the final time free.

198 A pay-off function J is defined as a function of the final state, $\mathbf{x}(t_f)$, and a

199 cost function $\mathcal{L}(t, \mathbf{x}(t), u(t))$ integrated from initial time (t_0) to final time (t_f).
200 Through choosing an optimal control $u^*(t)$ and solving for the corresponding
201 optimal state $\mathbf{x}^*(t)$, we seek to maximise or minimise this objective function.
202 Selecting the pay-off enables us to incorporate the context of our application
203 and determine the meaning of *optimality*. In general, the pay-off function can
204 be written as,

$$J = \phi(\mathbf{x}(t_f)) + \int_{t_0}^{t_f} \mathcal{L}(t, \mathbf{x}(t), u(t)) dt. \quad (8)$$

205 Depending on the form of ϕ , it may be possible to incorporate ϕ into \mathcal{L} by
206 restating the final state constraint in terms of an integral expression using
207 the Fundamental Theorem of Calculus, and noting that $\phi(\mathbf{x}(t_0))$ is constant
208 and hence does not impact the optimal control. The resulting unconstrained
209 optimal control problem is often more straightforward to solve than the con-
210 strained problem.

211 The optimal control can be found by solving necessary conditions obtained
212 through application of Pontryagin's Maximum Principle (PMP) [50], or a nec-
213 essary and sufficient condition by forming and solving the Hamilton-Jacobi-
214 Bellman partial differential equation; a dynamic programming approach [8]. In
215 this work we use the PMP and we construct the Hamiltonian, $H(t, \mathbf{x}, u, \boldsymbol{\lambda}) =$
216 $\mathcal{L}(t, \mathbf{x}, u) + \boldsymbol{\lambda}f$, where $\boldsymbol{\lambda} = [\lambda_1(t), \lambda_2(t), \dots, \lambda_n(t)]$ are the adjoint variables for
217 an n -dimensional state. The adjoint is analogous to Lagrange multipliers for
218 unconstrained optimisation problems. Through the Hamiltonian, the adjoint
219 allows us to link our state to our pay-off function. The necessary conditions
220 can be expressed in terms of the Hamiltonian,

221 (1) The optimality condition is obtained by minimising the Hamiltonian,
$$\frac{\partial H}{\partial u} = 0 \text{ gives } \left(\frac{\partial \mathcal{L}}{\partial u} + \boldsymbol{\lambda} \frac{\partial f}{\partial u} \right) = 0, \quad (9)$$

222 (2) the adjoint, also referred to as *co-state*, is found by setting,

224

$$\frac{\partial H}{\partial \mathbf{x}} = -\frac{d\boldsymbol{\lambda}}{dt}, \text{ giving } \frac{d\boldsymbol{\lambda}}{dt} = -\left(\frac{\partial \mathcal{L}}{\partial \mathbf{x}} + \boldsymbol{\lambda} \frac{\partial f}{\partial \mathbf{x}}\right), \text{ and} \quad (10)$$

225 (3) satisfying the transversality condition,

$$\boldsymbol{\lambda}(t_f) = \frac{\partial \phi}{\partial \mathbf{x}} \Big|_{t=t_f}. \quad (11)$$

227 4.2 Continuous optimal control

228 In this section we consider optimal control applied to the AML model pre-
 229 sented in Section 3. From this point we omit the implied time dependence of
 230 all control, state and co-state variables for notational convenience. Consider
 231 the steady states we observed for the coexistent parameter values of model
 232 1. Suppose we wish to apply an optimal control that steers the system from
 233 a steady state observed in Figure 4a towards a healthy steady state (Figure
 234 4b). This could be achieved by applying a drug $u(t)$, the dosage of which may
 235 vary over time, that kills leukaemic stem cells,

$$\begin{aligned} \frac{dS}{dt} &= \rho_S S(K_1 - Z_1) - \delta_S S, \\ \frac{dA}{dt} &= \delta_S S + \rho_A A(K_2 - Z_2) - \delta_A A, \\ \frac{dD}{dt} &= \delta_A A - \mu_D D, \\ \frac{dL}{dt} &= \rho_L L(K_2 - Z_2) - \delta_L L - \frac{\alpha L}{\gamma + L} - uL, \\ \frac{dT}{dt} &= \delta_L L - \mu_T T. \end{aligned} \quad (12)$$

236 A potential pay-off function for this optimal control problem is to minimise,

$$J = \int_0^{t_f} (a_1 u^2 + a_2 L^2) dt, \quad (13)$$

237 where the control problem is assumed to start at time zero and run until a
238 fixed end time of t_f . In defining a pay-off function there is significant scope
239 for flexibility, and what constitutes an appropriate choice depends on the
240 application. The parameters $a_1 > 0$ and $a_2 > 0$ are chosen to weight the
241 importance of each term in the pay-off, and can be adjusted to best suit a
242 particular application. Through scaling it can be seen that for this example
243 only the relative weighting (a_1/a_2) is important, however we specify a_1 and a_2
244 separately for clarity.

245 Quadratic pay-off functions have several desirable mathematical properties
246 that increase the ease of finding optimal solutions; they are smooth and have
247 only a single extremum. Furthermore, Quadratic pay-off functions help to
248 avoid non-physical controls that may otherwise be found. For example; if the
249 pay-off was a cubic function of u , setting u to be large and negative may min-
250 imise the pay-off but be physically unrealisable. Quadratic pay-off functions
251 also have some desirable physical properties; a quadratic term will apply a
252 harsher penalty to large amounts of control than small amounts [5], which in
253 many treatments, such as chemotherapy, is desirable [29]. In control engineer-
254 ing applications, the control, u , is thought to be proportional to a voltage or
255 current, in which case a quadratic pay-off has a convenient interpretation, as
256 u^2 is proportional to power, and the integral of this power over an interval is
257 proportional to the energy expended [5]. Pay-off functions that are quadratic
258 in the control variable are used in many biological [38,53] and engineering
259 applications [3,48].

260 We can construct the Hamiltonian as $H = \mathcal{L} + \boldsymbol{\lambda}f$; where f is the right hand
261 side of Equation (12), $\boldsymbol{\lambda} = [\lambda_1, \lambda_2, \lambda_3, \lambda_4, \lambda_5]$, and from Equation (13), we have

262 $\mathcal{L} = a_1 u^2 + a_2 L^2$, giving,

$$\begin{aligned}
 H &= a_2 L^2 + a_1 u^2 + \lambda_1 [\rho_S S(1 - S) - \delta_S S] \\
 &+ \lambda_2 [\delta_S S + \rho_A A(1 - A - L) - \delta_A A] \\
 &+ \lambda_3 (\delta_A A - \mu_D D) \\
 &+ \lambda_4 [\rho_L L(1 - A - L) - \delta_L L - \alpha L / (\gamma + L) - uL] \\
 &+ \lambda_5 (\delta_L L - \mu_T T). \tag{14}
 \end{aligned}$$

263 From Equation (9), we find the optimal control by setting $\partial H / \partial u = 0$, giving
 264 $u^* = \lambda_4 L / 2a_1$. Following Equation (10), the co-state equations for $\boldsymbol{\lambda}$ are found
 265 by setting $d\boldsymbol{\lambda} / dt = -\partial H / \partial \mathbf{x}$,

$$\begin{aligned}
 \frac{d\lambda_1}{dt} &= 2S\lambda_1\rho_S + \delta_S\lambda_1 - \delta_S\lambda_2 - \lambda_1\rho_S, \\
 \frac{d\lambda_2}{dt} &= 2A\lambda_2\rho_A + L\lambda_2\rho_A + L\lambda_4\rho_L + \delta_A\lambda_2 - \lambda_2\rho_A, \\
 \frac{d\lambda_3}{dt} &= \mu_D\lambda_3, \\
 \frac{d\lambda_4}{dt} &= -2a_2L + \rho_AA\lambda_2 + \lambda_4\rho_LA + 2\rho_LL\lambda_4 - \lambda_4\rho_L, \\
 &+ \lambda_4\delta_L + \frac{\alpha\gamma\lambda_4}{(\gamma + L)^2} + \lambda_4u - \gamma_L\lambda_5, \\
 \frac{d\lambda_5}{dt} &= \mu_T\lambda_5. \tag{15}
 \end{aligned}$$

266 The transversality condition, Equation (11), gives final time conditions on
 267 the co-state, Equation (15); $\boldsymbol{\lambda}(t_f) = [0, 0, 0, 0, 0]$. Assuming that the initial
 268 state is known; $[S(0), A(0), D(0), L(0), T(0)]$, it is now possible to determine
 269 the optimal control and corresponding state and co-state through solving a
 270 two-point boundary value problem (BVP).

271 We solve Equation (2) numerically to reach the stable coexistence steady state

272 of the uncontrolled model. These steady state values in the absence of the
273 control are used as the initial state conditions to solve the BVP to find the
274 optimal control solution. The initial condition for the optimal control prob-
275 lem is $[S(0), A(0), D(0), L(0), T(0)] = [0.7200, 0.3255, 0.5207, 0.3715, 0.0619]$.
276 Initialising the optimal control solution from the uncontrolled steady state is
277 not necessary, however it helps to illustrate the role of the control.

278 There are a range analytical methods available for solving some forms of BVP
279 under certain restrictions conditions [1,62]. However, in this work we focus on
280 numerical solutions with a view to identifying and discussing typical issues
281 that may arise in implementation. Common numerical solution techniques
282 include shooting and forward backward sweep methods (FBSM) [27,36]. The
283 most effective numerical method depends on the particular BVP. The single
284 shooting method is relatively straightforward, but can be sensitive to the initial
285 guess of the co-state. Forming a suitable guess for the initial values of the co-
286 state is challenging, as the co-state does not have a straightforward physical
287 interpretation. Although the FBSM calls for an initial guess for the control
288 over the entire interval, this can often be straightforward to determine, as we
289 will demonstrate.

290 We apply the FBSM using an initial guess for the control, $u(t) \equiv 0$, to solve
291 for the state variables forward in time. The co-state is then solved backward
292 in time. In each case a fixed step fourth order Runge-Kutta method is applied
293 to solve the relevant system of ODEs. Using these solutions, the control is up-
294 dated and the process is repeated until convergence is achieved. The algorithm
295 for the forward-backward sweep method is given in Algorithm 1.

Algorithm 1: Forward-backward sweep

- i. Make an initial guess of $u(t)$.

Typically $u(t) \equiv 0$ is sufficient, though a more thoughtful choice may result in fewer iterations required for convergence.

- ii. Using the initial condition $\mathbf{x}(0) = \mathbf{x}_0$, solve for $\mathbf{x}(t)$ forward in time using the initial guess of $u(t)$.

- iii. Using the transversality condition $\boldsymbol{\lambda}(t_f)$, solve for $\boldsymbol{\lambda}(t)$ backwards in time, using the values for $u(t)$ and $\mathbf{x}(t)$.

- iv. Calculate $u_{\text{new}}(t)$ by evaluating the expression for the optimal control $u^*(t)$ using the updated $\mathbf{x}(t)$ and $\boldsymbol{\lambda}(t)$ values.

- v. Update $u(t)$ based on a combination of $u_{\text{new}}(t)$ and the previous $u(t)$.

For continuous controls applied to relatively simple systems, it may be possible to use $u_{\text{new}}(t)$ directly ($u(t) = u_{\text{new}}(t)$), however this is not sufficient to achieve convergence in general. We discuss this further in Section 4.4.

- vi. Check for convergence.

If $\mathbf{x}(t)$, $\boldsymbol{\lambda}(t)$ and $u(t)$ are within a specified absolute or relative tolerance of the previous iteration, accept $\mathbf{x}(t)$, $\boldsymbol{\lambda}(t)$ and $u(t)$ as having converged, otherwise return to Step ii. and repeat the process using the updated $u(t)$.

296 Solutions are provided in Figure 5 for various weighting on the control param-
297 eters. As expected, when $a_1 > a_2$, placing a greater weighting on the negative
298 impact of the control than the negative impact of the leukaemic stem cells we
299 observe that the control is applied at a lower level than when $a_1 < a_2$. When
300 the pay-off weightings are equal, as shown in Figure 5b, the continuous control
301 is applied at an amount similar to the level of the leukaemic stem cell popula-
302 tion. Similarly, when the amount of control applied is larger, we observe that
303 the leukaemic stem cell population declines at a faster rate. With $a_1 > a_2$, as
304 in Figure 5c, we observe that the leukaemic population is effectively eradicated

305 by t_f , whereas when $a_1 < a_2$ we see, in Figure 5d, that a leukaemic population
306 remains at t_f . A limitation of specifying a fixed final time, as opposed to a
307 fixed final state, is that the optimal outcome is dependent on the specified final
308 time, and there is no consideration for what may happen *after* t_f . In many
309 applications, the notion of what happens beyond the control interval is not of
310 interest, though in some instances specifying a final state may be more sensi-
311 ble. In this work we consider fixed final time problems for ease of comparison
312 between controls under different parameter regimes, though we acknowledge
313 that specifying a final state, such as *no leukaemic stem cells*, may be more
314 biologically appropriate.

315 For each of the optimal controls presented in Figure 5, we include an estimate
316 of J , calculated by evaluating Equation (13) with the trapezoid rule. It is
317 critical to note that these pay-offs should not be directly compared with each
318 another. This kind of comparison would be meaningless as each result corre-
319 sponds to different choices of a_1 and a_2 , and these values explicitly contribute
320 to J . For example; suppose an optimal control with pay-off weightings a_1 and
321 a_2 is computed to have a pay-off of J_1 . Recomputing the optimal control with
322 weightings $2a_1$ and $2a_2$ would produce a near identical optimal control and
323 corresponding state, with slight deviation due to floating-point error. However,
324 the corresponding pay-off J_2 would be twice as large.

325 No pay-off is calculated for the uncontrolled steady state solution (Figure 5a)
326 as the choice of a_1 and a_2 would be arbitrary. In this sense, computed pay-offs
327 are not useful for comparing the outcome of *treatment* versus *no treatment* as
328 there is no meaningful pay-off associated with no treatment. Rather, computed
329 pay-offs can be used for comparison with other controls applied to a system
330 with identical parameters to check whether or not they are comparable in
331 outcome to the optimal control, noting that the response of the state will also
332 change if the control changes.

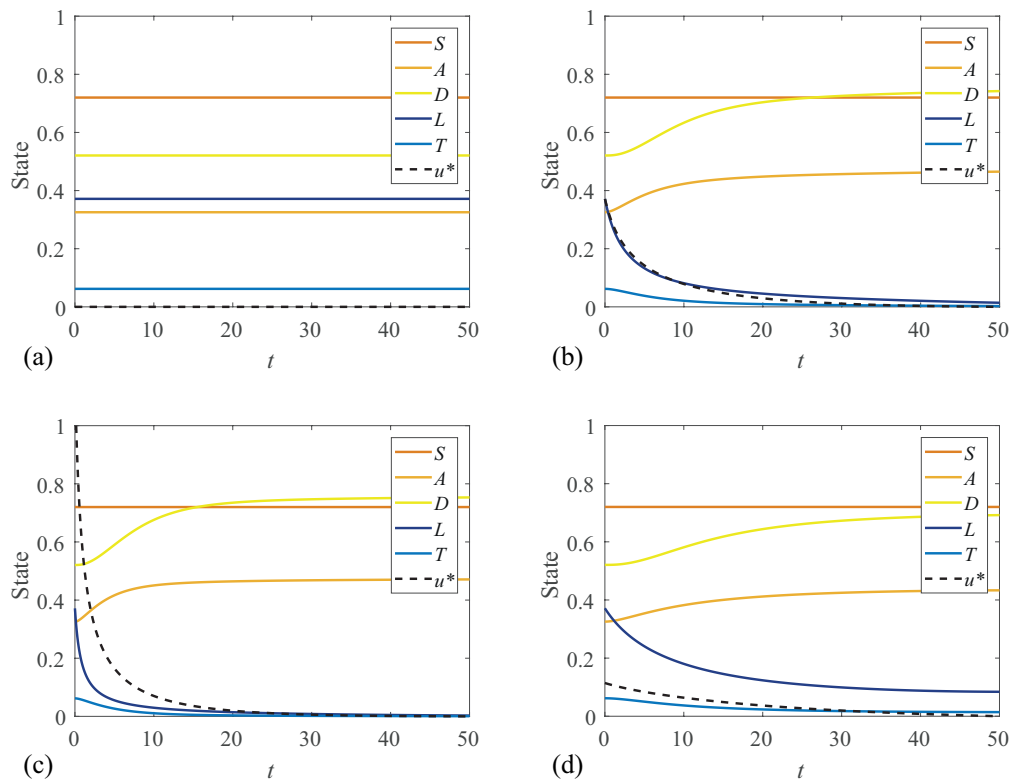


Fig. 5. Application of a continuous optimal control (black dashed line) for various pay-off weightings a_1 and a_2 . The corresponding pay-off, J , is also given. (a) Coexisting steady state solution with no control applied. (b) Equal weighting $[a_1, a_2] = [1, 1]$, $J = 0.7167$. (c) Leukaemia weighted more heavily $[a_1, a_2] = [0.1, 1]$, $J = 0.2288$. (d) Control weighted more heavily $[a_1, a_2] = [1, 0.1]$, $J = 0.2262$. These figures are produced with immune response parameters $\alpha = 0.015$, $\gamma = 0.1$.

333 4.3 *Bang-bang optimal control*

334 In addition to considering continuous controls, it is also relevant to con-
 335 sider discontinuous bang-bang controls as this kind of *on-off* control could
 336 be thought to be more clinically relevant than a continuous setting. Bang-
 337 bang control problems require a specified bound on the control variable. A
 338 bang-bang optimal control takes the value of either the upper or lower bound
 339 with finitely many switching points over an interval. As a starting point we
 340 re-consider Equation (12) and note that a control will be either bang-bang op-
 341 timal or singular if the pay-off function is linear in the control term. A pay-off
 342 that should produce a bang-bang or singular optimal control of Equation (12)
 343 is to minimise

$$J = \int_0^{t_f} (a_1 u + a_2 L) dt, \quad (16)$$

344 subject to $b_1 \leq u \leq b_2$. We can construct the Hamiltonian as $H = \mathcal{L} + \boldsymbol{\lambda} f$,
 345 where \mathcal{L} is the integrand of Equation (16), $\boldsymbol{\lambda} = [\lambda_1, \lambda_2, \lambda_3, \lambda_4, \lambda_5]$ and f is the
 346 right hand side of Equation (12), giving

$$\begin{aligned} H = & a_2 L + a_1 u + \lambda_1 [\rho_S S(1 - S) - \delta_S S] \\ & + \lambda_2 [\delta_S S + \rho_A A(1 - A - L) - \delta_A A] \\ & + \lambda_3 (\delta_A A - \mu_D D) \\ & + \lambda_4 [\rho_L L(1 - A - L) - \delta_L L - \alpha L / (\gamma + L) - uL] \\ & + \lambda_5 (L\delta_L - T\mu_T). \end{aligned} \quad (17)$$

347 As for the continuous control case, we differentiate the Hamiltonian with re-
 348 spect to our control variable u . With a linear pay-off, however, the result no
 349 longer contains u . Rather than solving for u , we define a switching function,

350 $\psi(t)$, given by

$$\psi(t) = \frac{\partial H}{\partial u} = -\lambda_4(t)L(t) + a_1. \quad (18)$$

351 From PMP [50], it is implied that the Hamiltonian will be minimised under
352 the following conditions,

$$u^*(t) = \begin{cases} b_1, & \text{if } \psi(t) > 0, \\ b_2, & \text{if } \psi(t) < 0. \end{cases} \quad (19)$$

353 Conditions in Equation (19) produce a bang-bang control. Here, the control
354 variable takes a value of either its upper or lower bound. Notably, Equation
355 (19) omits the case where $\psi(t) = 0$, as a bang-bang optimal control requires
356 that $\psi(t) = 0$ only at discrete points, if at all [13]. If $\psi(t) = 0$ for any finite
357 interval aside from isolated points, the control is singular. Singular controls are
358 most commonly encountered in cases where the Hamiltonian is linear in the
359 control variable but non-linear in some state variables [11]. When $\psi(t) = 0$ over
360 an interval, the Hamiltonian is not a function of the control, so the state and
361 co-state variables no longer determine the control [11]; over this interval the
362 control is determined by requiring $\partial H/\partial u = 0$. Our control problem defined by
363 Equation (12) and Equation (16) is not singular, so we do not discuss singular
364 controls further.

365 Our co-state equations for λ are found as $\partial H/\partial f = -d\lambda/dt$. The co-state in

366 the bang-bang control problem is given by,

$$\begin{aligned}
 \frac{d\lambda_1}{dt} &= 2S\lambda_1\rho_S + \delta_S\lambda_1 - \delta_S\lambda_2 - \lambda_1\rho_S, \\
 \frac{d\lambda_2}{dt} &= 2A\lambda_2\rho_A + L\lambda_2\rho_A + L\lambda_4\rho_L + \delta_A\lambda_2 - \lambda_2\rho_A, \\
 \frac{d\lambda_3}{dt} &= \mu_D\lambda_3, \\
 \frac{d\lambda_4}{dt} &= -a_2 + \rho_AA\lambda_2 + \lambda_4\rho_LA + 2\rho_LL\lambda_4 - \lambda_4\rho_L \\
 &\quad + \lambda_4\delta_L + \frac{\alpha\gamma\lambda_4}{(\gamma + L)^2} + \lambda_4u - \gamma_L\lambda_5, \\
 \frac{d\lambda_5}{dt} &= \mu_T\lambda_5,
 \end{aligned} \tag{20}$$

367 and we note that Equation 20 is subtly different to Equation 15, as the first
 368 term of the fourth line of Equation (20) is the constant $-a_2$, and no longer
 369 depends on L .

370 The transversality condition, Equation (11), gives the final time conditions
 371 on the co-state, $[\lambda_1(t_f), \lambda_2(t_f), \lambda_3(t_f), \lambda_4(t_f), \lambda_5(t_f)] = [0, 0, 0, 0, 0]$. Assuming
 372 again that the initial state is known; $[S(0), A(0), D(0), L(0), T(0)]$, it is now
 373 possible to determine the optimal bang-bang control and corresponding opti-
 374 mal state and co-state through solving a two-point BVP that we solve using
 375 the FBSM, as in the continuous control case. It is not necessary to modify
 376 the FBSM algorithm to find bang-bang optimal controls, though care must
 377 be taken in how the control is updated between iterations. This is discussed
 378 further in Section 4.4. Depending on the numerical scheme used to integrate
 379 the state and co-state equations through time, the discontinuous nature of
 380 the bang-bang control may require careful handling. Solutions are provided in
 381 Figure 6 for various weighting on the control parameters. In the continuous
 382 control case, when $a_1 > a_2$, placing a greater weighting on the negative im-
 383 pact of the control than the negative impact of the leukaemic stem cells; we
 384 observed that the control is applied at a lower level than when $a_1 < a_2$. The
 385 optimal bang-bang control must take either the upper or lower bound of the

386 specified range. As such, in the bang-bang control case the pay-off weighting
 387 parameters determine not the level at which the control is applied, but rather
 388 the times at which the control switches from one bound to the other, hence
 389 the name *switching function* given to Equation (19).

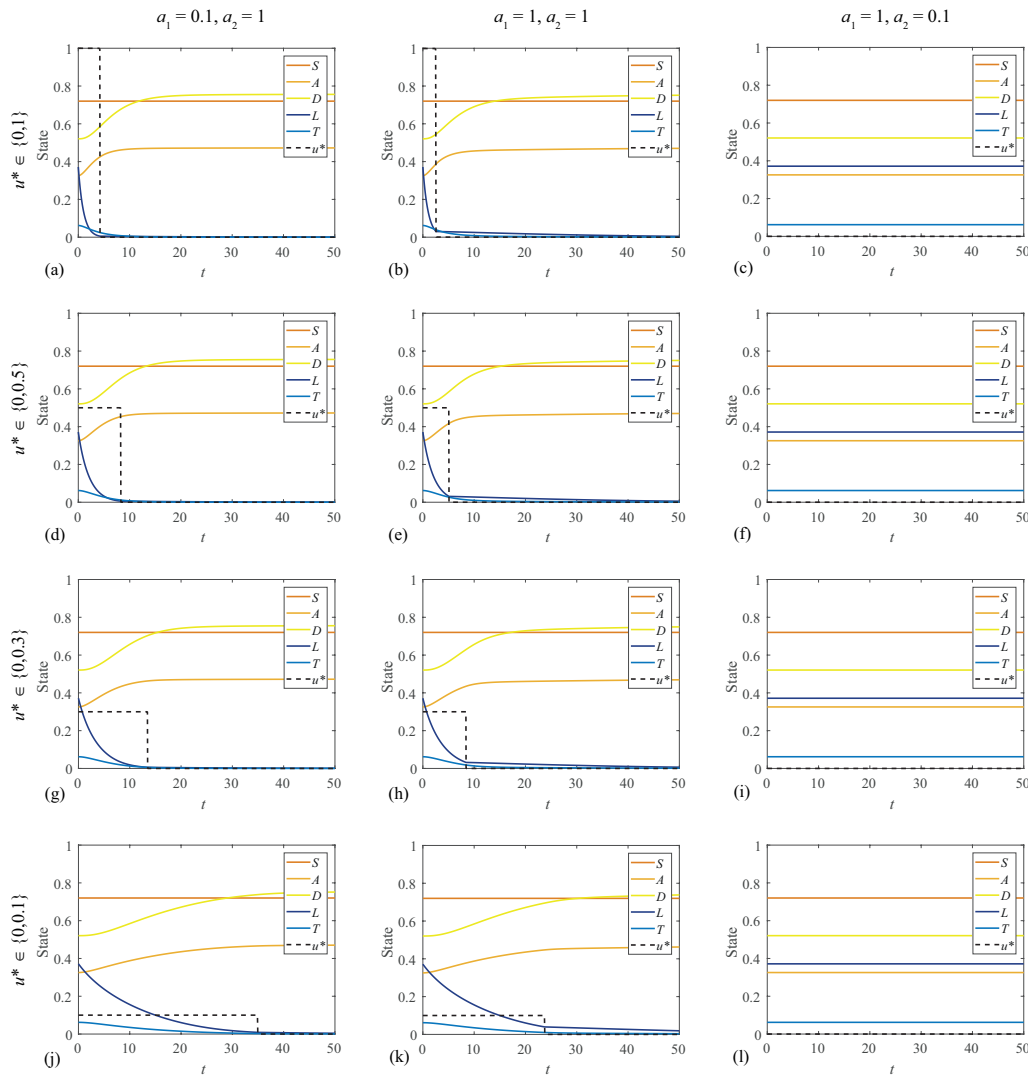


Fig. 6. Bang-bang control solutions for various weightings on control and leukaemia in the pay-off (a_1 and a_2 respectively), with different control upper bounds. These figures are produced with immune response parameters $\alpha = 0.015$, $\gamma = 0.1$.

390 In Figure 6 it is clear that when the upper bound on the control is higher,
 391 meaning in this context the maximum amount of chemotherapy that can be
 392 applied at any given time is higher, the control switches to the lower bound
 393 earlier. In this case the lower bound corresponds to $u = 0$, or no chemotherapy

394 being applied (control *switched off*), though this is not required of the method.
395 The interaction between the control and state in Equation (20) means that
396 the cumulative amount of control applied is not the same for different bounds
397 on the control. In Figure 5 we demonstrate that for a continuous control with
398 $a_1 = 1$, $a_2 = 0.1$, a small amount of control is applied. For the bang-bang case
399 with the same weighting, we observe in the rightmost column of Figure 6 that
400 for a range of control upper bounds, the control is not switched on at all -
401 implying that with such a pay-off, it is optimal not to apply the control. One
402 may suppose that for a sufficiently small upper bound that the control would
403 turn on even with this pay-off, however a lower upper bound on the control
404 also reduces the impact the control has on the state.

405 Due to the immune response incorporated in Section 3, a sufficiently small
406 leukaemic population will tend towards extinction rather than grow back to
407 a coexisting steady state. Because of this, we observe in Figure 6 that the
408 control switches off before the leukaemic stem cells are totally eradicated -
409 the immune response is sufficient once the leukaemic population is sufficiently
410 low. This is most evident in Figure 6k, where we can see that the population
411 of leukaemic stem cells is declining but has not become extinct by the final
412 time, $t = 50$. In absence of the immune response incorporated in Section 3, we
413 would observe the leukaemic population increasing as soon as the control is
414 switched off, since the healthy steady state would be unstable; applying fixed
415 final time bang-bang optimal control to the original model produces outcomes
416 that are mathematically optimal but physically undesirable.

417 In our discussion of continuous controls, we note the fixed final time as a
418 limitation, since changing the final time can change the profile of the optimal
419 control and state. In general the same is true of bang-bang controls with fixed
420 final times, though in some instances that we consider the optimal bang-bang
421 control does not change significantly if the final time is changed. For example;
422 the optimal switching times and corresponding optimal states in the leftmost

423 column of Figure 6 do not change significantly if the final time is increased to
424 $t = 100$, because by $t = 50$ we see that $L \approx 0$ and $u = 0$, so neither contributes
425 significantly to the pay-off in the interval $50 < t \leq 100$. For these cases the
426 control is not costly relative to the leukaemia ($a_1 < a_2$) so it is applied at the
427 upper bound until the leukaemic stem cell population is virtually eradicated
428 before switching off.

429 For this particular system, we only obtain bang-bang optimal controls with a
430 single switching time. We are able to verify these bang-bang optimal controls
431 through an exhaustive search of all possible bang-bang controls by specifying
432 the switching time, directly calculating the pay-off and determining the
433 switching time that minimises the pay-off. For all cases considered in Figure 6
434 the switching time identified via exhaustive search is in agreement. It is also
435 possible that the optimal bang-bang control may switch between the upper
436 and lower bounds numerous times, producing multiple ‘bangs’. Bang-bang op-
437 timal controls that exhibit multiple bangs can be identified using the FBSM
438 without modification, though it is more difficult to find a convergent bang-
439 bang optimal control with multiple bangs. Similarly, without knowing a priori
440 how many switching times to expect, an exhaustive search for multiple bangs
441 is not computationally feasible.

442 *4.4 Convergence and control updating*

443 In this section we examine the convergence behaviour of solutions to the op-
444 timal control problems presented in this work. Convergence behaviour of nu-
445 merical solutions to optimal control problems is influenced by multiple factors.
446 In particular, we discuss the initial guess of the control, convergence criteria,
447 control updating and pay-off weightings. These factors influence not only the
448 number of iterations required to reach a converged numerical solution, but
449 also whether or not a converged solution will be reached at all.

450 Holding all other factors constant, provided that the initial guess for the con-
451 trol is sensible, the initial guess does not have a significant impact on whether
452 or not a converged result is reached for the control problems considered in this
453 work. However, convergence is typically reached with fewer iterations when the
454 initial guess is relatively closer to the true value of the optimal control. For
455 simplicity we use the initial guess $u \equiv 0$ for all results presented in this work,
456 while acknowledging that more thoughtful choices may deliver convergence in
457 fewer iterations.

458 For optimal control results presented in the previous sections, we determine
459 whether convergence has been achieved after each iteration based on the rela-
460 tive difference between the updated control, u_{updated} , and the old control, u_{old} .
461 If this relative difference is sufficiently small, the updated control is accepted
462 as the optimal control. A typical relative difference convergence criterion re-
463 quires

$$\frac{|u_{\text{updated}} - u_{\text{old}}|}{|u_{\text{updated}}|} \leq \varepsilon, \quad (21)$$

464 where $0 < \varepsilon \ll 1$ is the desired relative tolerance. Following [36], we adjust
465 Equation (21) to allow for a control of the form $u \equiv 0$, giving

$$\varepsilon \sum_{i=1}^n |u_{\text{updated}}(i\Delta t)| - \sum_{i=1}^n |u_{\text{updated}}(i\Delta t) - u_{\text{old}}(i\Delta t)| \geq 0, \quad (22)$$

466 where $t = i\Delta t$, Δt is the numerical time step and n is the number of nodes
467 in the time discretisation. The absolute value is taken to ensure that positive
468 differences are not offset by negative differences that could otherwise result
469 in incorrectly detecting convergence. The choice of convergence criterion and
470 acceptable tolerance depends on the particular problem at hand, and may
471 need to be adjusted to be appropriate for another control problem. In some
472 instances, it may be necessary to check convergence of the state and co-state
473 as well as the control, particularly if the state response to control is sensitive.

474 For the control problems studied in this work, we find that state and co-
475 state respond predictably to the control, and convergence of the control is
476 accompanied by convergence of that state and co-state. As such we do not
477 explicitly check for convergence of the state and co-state.

478 In each iteration of the FBSM we recalculate the control, u_{new} , based on the
479 newly calculated state and co-state solutions and associated optimality cri-
480 terion, as discussed in Section 4.2 for the continuous control and Section 4.3
481 for the bang-bang control. Typically, u_{new} is not used directly as the control
482 for the next iteration of the FBSM, but rather we form an updated control
483 u_{updated} as a weighted combination of u_{new} and the control from the previ-
484 ous iteration, u_{old} . The motivation for this is two-fold; first, an appropriately
485 weighted control updating scheme can speed up convergence; and second, for
486 many optimal control problems, a direct update of $u_{\text{updated}} = u_{\text{new}}$ will fail
487 to produce converging results at all. A common approach is to update the
488 control based on a convex combination, such that the total weightings sum to
489 one, of the new and previous control(s). In this work we use a constant linear
490 weighting, with $0 < \omega < 1$, giving

$$u_{\text{updated}} = \omega u_{\text{old}} + (1 - \omega) u_{\text{new}}. \quad (23)$$

491 We find that the best choice for ω depends not only on the form of the control,
492 continuous or bang-bang, but also on model parameters such as the pay-off
493 weightings. There is a trade-off between the number of iterations required to
494 obtain convergence, and actually converging at all; a larger ω typically is more
495 likely to produce converging solutions, but this also means that the control
496 changes less each iteration, so more iterations are required. For example, a
497 weighting of $\omega = 0.7$ was sufficiently large that all continuous control solutions
498 presented in Figure 5 converged to a relative tolerance of $\varepsilon = 1 \times 10^{-3}$. For
499 $\omega = 0.6$ only Figure 5d converges, and for $\omega = 0.8$, all solutions in Figure 5

500 converge but require more iterations than when $\omega = 0.7$.

501 Convergence in the bang-bang control case typically requires larger ω and more
502 iterations than the continuous controls. In the rightmost column of Figure
503 6, there is no concept of convergence as the control never switches on. Only
504 Figure 6j and Figure 6k converge to a relative tolerance of 1×10^{-3} for $\omega = 0.7$,
505 with $\omega = 0.9$ being sufficient for convergence of all remaining solutions aside
506 from Figure 6b, where we set $\omega = 0.95$.

507 It is clear that the best control updating scheme depends on the particular
508 problem; and a scheme that works well for one problem may not necessarily
509 work at all for another. When solving control problems, it may be necessary
510 to try a range of updating schemes to achieve convergence. In this work we
511 only consider constant weighted updating, though there are more sophisti-
512 cated updating schemes that shift the weighting towards u_{new} as the number
513 of iterations increase [36]. In Figure 7 we examine the influence of the control
514 update weighting ω , and the pay-off weightings, a_1 and a_2 , on the convergence
515 behaviour of the bang-bang control problem studied in Section 4.3. Specifi-
516 cally, we consider the case where $0 \leq u \leq 0.5$, and determine that a solution
517 has converged if it meets a relative tolerance of $\varepsilon = 1 \times 10^{-3}$ within 250 it-
518 erations. In each panel of Figure 7 we observe three *regions*: in region I we
519 have no concept of convergence as the control never switches on; in region II
520 we find that the optimal control problem does not converge; and in region III
521 we observe convergence. Not all simulations conform strictly to these regions
522 since the boundary between the different regions is not always sharp and well-
523 defined. However, broadly speaking, these three regions capture the essence
524 of the convergence behaviour that we observe. These regions are constructed
525 based on discrete simulations of the problem for $0 < a_1 \leq 10$ and $0 \leq a_2 \leq 10$,
526 each in increments of 0.1. The case where $a_1 = 0$ is excluded as this corre-
527 sponds to no cost associated with applying the control, so there is no sense of
528 convergence.

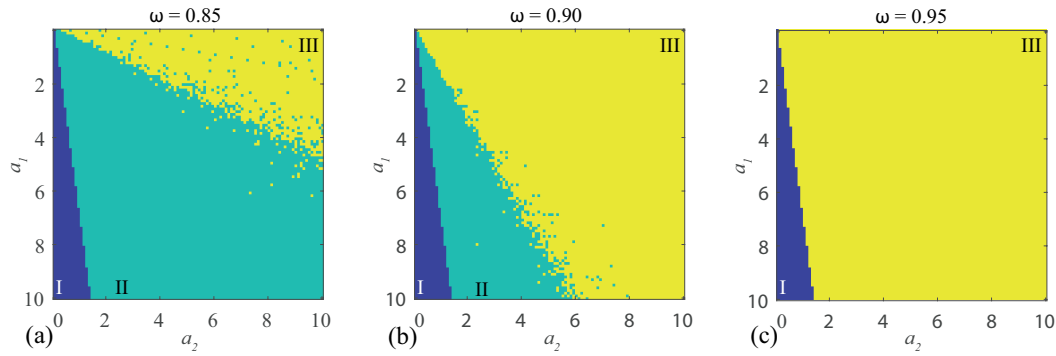


Fig. 7. Convergence behaviour for (a) $\omega = 0.85$, (b) $\omega = 0.9$, and (c) $\omega = 0.95$, with a_1 and a_2 ranging from 0 to 10 in increments of 0.1, excluding $a_1 = 0$. In region I (dark blue) we have no concept of convergence as the control never switches on. In region II (light blue) we find that the optimal control problem does not converge, and in region III (yellow) we observe convergence. These figures are produced with immune response parameters $\alpha = 0.015$, $\gamma = 0.1$.

529 From Figure 7 it is clear that convergence is achieved in a larger region of the
530 (a_1, a_2) parameter space when ω is increased. However, it is important to note
531 that achieving convergence in this context only implies that Equation (22) is
532 satisfied, and does not necessarily mean that a suitable bang-bang control is
533 obtained. While some controls corresponding to individual simulations in Fig-
534 ure 7c are suitable bang-bang controls; a portion are approaching bang-bang
535 but require additional iterations to accurately calculate the control around
536 the switching point. The weighting applied in Equation (23) has the effect
537 of smoothing u during intermediate iterations of the FBSM; this smoothness
538 is gradually reduced as the control converges to the optimal switching point.
539 Since ω explicitly influences the relative amount that the control can differ
540 between iterations, if a larger ω is required to achieve convergence for a given
541 problem, it may also be necessary to reduce the convergence tolerance ε to
542 ensure that the resulting control is sufficiently bang-bang.

543 5 Conclusion and Outlook

544 In this work we consider a haematopoietic stem cell model of AML that incor-
545 porates competition between leukaemic stem cells and blood progenitor cells
546 within the bone marrow niche. We incorporate a biologically appropriate im-
547 mune response in the form of a Michaelis-Menten term. This modification is
548 mathematically convenient because of the impact it has on the steady states,
549 and biologically relevant because the immune response is known to play an
550 important role in cancer progression and treatment. With a view to identify-
551 ing the optimal way to apply a treatment such as chemotherapy to the model,
552 we formulate and solve optimal control problems corresponding to multiple of
553 objectives and constraints. This includes quadratic pay-off functions, yielding
554 continuous controls, as well as linear pay-off functions, yielding discontinuous
555 bang-bang controls.

556 We provide a brief overview of optimal control theory, with a focus on the
557 necessary conditions derived from Pontryagin's Maximum Principle. This ap-
558 proach formulates the optimal control problem as a coupled multi-species
559 two-point boundary value problem. The resulting optimal control problem
560 is solved numerically using the iterative FBSM. The algorithm for the FBSM
561 is discussed, with a focus on highlighting typical issues that may arise in im-
562 plementing optimal control. Suggestions are provided for overcoming these
563 issues. In particular, we focus on factors that influence the convergence of
564 the FBSM; not only in terms of the number of iterations required, but also
565 whether it converges at all. These factors include the initial guess for the
566 control, the convergence criterion, the method of updating the control, the
567 associated weighting placed on controls from prior iterations and parameters
568 such as pay-off weightings, and in the bang-bang control case, the control
569 bounds.

570 For the model we consider; a well informed initial guess for the control may re-

571 duce the number of iterations required for convergence, but any sensible guess
572 should not prevent convergence. Most critically, we show that the method of
573 updating the control and the associated weight placed on the control from the
574 previous iteration has a significant impact on whether or not convergence will
575 be achieved, as do the weights in the pay-off function. In the bang-bang control
576 case, we observe that increasing the upper bound on the control can prevent
577 convergence, holding all other factors constant; in this case, placing a greater
578 weight on the solution from the previous iteration may produce convergence.

579 There are many potential avenues to extend the ideas explored in this work.
580 Here, we have incorporated the control via a simple mechanism, and more so-
581 phisticated pharmacokinetic processes such as drug absorption and metabolism
582 could be incorporated to increase the biological detail captured by the model,
583 but this additional biological detail comes at the cost of increasing the num-
584 ber of unknown, and possibly unmeasurable parameters. Therefore, care must
585 be exercised in following up this kind of extension. The control problems pre-
586 sented in this work could be reformulated as fixed final state problems, leaving
587 the final time free to vary which could be more clinically relevant than spec-
588 ifying the final time. With the introduction of an immune mechanism to the
589 model, it is also possible to consider a control based around immunotherapy.

590 A recent idea of great interest in clinical cancer research is the possibility of
591 introducing an interval of time during treatment in which no chemotherapy is
592 applied. This kind of intervention is reminiscent of a bang-bang control, and
593 is often referred to as a *drug holiday* [59]. There is some evidence to suggest
594 that drug resistance of tumour cells may reduce with time so that patients
595 experience an improve response to chemotherapy following a drug holiday
596 [32,33,54]. This application of a drug in an *on-off* fashion parallels the idea of
597 the bang-bang controls we consider in this work and so it would be interesting
598 to formulate the concept of designing a drug holiday in terms of a bang-bang
599 optimal control problem using the algorithms and concepts developed in this

600 work.

601 *Acknowledgments.* This work is supported by the United States Air Force
602 Office of Scientific Research (BAA-AFRL-AFOSR-2016-0007) and the Aus-
603 tralian Research Council (DP170100474). Computational resources were pro-
604 vided by the eResearch Office at QUT.

605 **References**

- 606 [1] Adomian, G., Rach, R., 1993. Analytic solution of nonlinear boundary-value
607 problems in several dimensions by decomposition. *J Math Anal Appl.* 174: 118–
608 137.
- 609 [2] Almcera, A.E.S., Nguyen, V.K., Hernandez-Vargas, E.A., 2018. Multiscale
610 model within-host and between-host for viral infectious diseases. *J Math Biol.*
611 19: 1–23.
- 612 [3] Anderson, B., Moore, J., 2014. *Optimal Control Linear Quadratic Methods.*
613 Dover Publications, New York.
- 614 [4] Andreeff, M., 2015. *Current Cancer Research: Targeted Therapy of Acute*
615 *Myeloid Leukaemia.* Springer-Verlag, New York.
- 616 [5] Athans M., Falb, P., 1966. *Optimal Control: An Introduction to the Theory and*
617 *its Applications.* McGraw-Hill, New York.
- 618 [6] Austin, R., Smyth, M.J., Lane, S.W., 2016. Harnessing the immune system in
619 acute myeloid leukaemia. *Critical Reviews in Oncology/Hematology.* 103: 62–77.
- 620 [7] Australian Institute of Health and Welfare, 2014. *Cancer in Australia: an*
621 *overview 2014.* Canberra: AIHW.
- 622 [8] Bellman, R.E., 1957. *Dynamic Programming.* Princeton University Press,
623 Princeton.

- 624 [9] Boddu, P., Kantarjian, H., Garcia-Manero, G., Allison, J., Sharma, P., Daver,
625 N., 2018. The emerging role of immune checkpoint based approaches in AML and
626 MDS. *Leuk Lymphoma*. 59: 790–802.
- 627 [10] Burnett, A.K., 2001. *Clinical Haematology: Acute Myeloid Leukaemia*. Baillière
628 Tindall, London.
- 629 [11] Bryson, A., Ho, Y.C., 1975. *Applied Optimal Control: Optimization,*
630 *Estimation, and Control*. Taylor & Francis, Abingdon.
- 631 [12] Byrne, H.M., 2010. Dissecting cancer through mathematics: from the cell to the
632 animal model. *Nat Rev Cancer*. 10: 221–230.
- 633 [13] Carmichael, D.G., 1990. Bang-bang control and optimum structural design.
634 *Engineering Optimization*. 15: 205–209.
- 635 [14] Castiglione, F., Piccoli, B., 2007. Cancer immunotherapy, mathematical
636 modeling and optimal control. *J Theor Biol*. 247: 723–732.
- 637 [15] Castro, M., Lythe, G., Molina-Paris, C., Ribeiro, R.M., 2016. Mathematics in
638 modern immunology. *Interface Focus*. 6: 20150093.
- 639 [16] Chamchod, F., 2018. Modeling the spread of capripoxvirus among livestock and
640 optimal vaccination strategies. *J Theor Biol*. 437: 179–186.
- 641 [17] Corthay, A., 2014. Does the immune system naturally protect against cancer?
642 *Frontiers in Immunology*. 5: 197.
- 643 [18] Cucuianu, A., Precup, R., 2010. A hypothetical-mathematical model of acute
644 myeloid leukaemia pathogenesis. *Comput Math Methods Med*. 2010: 49–65.
- 645 [19] Day, C., Merlino, G., Dyke, T.V., 2015. Preclinical mouse cancer models: a
646 maze of opportunities and challenges. *Cell*. 163: 39–53.
- 647 [20] Döhner, H., Estey, E.H., Amadori, S., Appelbaum, F.R., Büchner, T., Burnett,
648 A.K., Dombret, H., Fenaux, P., Grimwade, D., Larson, R.A., Lo-Coco, F., Naoe,
649 T., Niederwieser, D., Ossenkoppele, G.J., Sanz, M.A., Sierra, J., Tallman, M.S.,
650 Löwenberg, B., Bloomfield, C.D., 2010. Diagnosis and management of acute

651 myeloid leukemia in adults: recommendations from an international expert panel,
652 on behalf of the European LeukemiaNet. *Blood*. 115: 453–474.

653 [21] Crowell, H.L., MacLean, A.L., Stumpf, M.P.H., 2016. Feedback mechanisms
654 control coexistence in a stem cell model of acute myeloid leukaemia. *J Theor Biol*.
655 401: 43–53.

656 [22] Estey, E., Döhner, H., 2006. Acute myeloid leukaemia. *Lancet*. 368: 1894–1907.

657 [23] Fribourg, M., Hartmann, B., Schmolke, M., Marjanovic, N., Albrecht, R.A.,
658 Garca-Sastre, A., Sealfon, S.C., Jayaprakash, ., Hayot, F., 2014. Model of influenza
659 A virus infection: dynamics of viral antagonism and innate immune response. *J*
660 *Theor Biol*. 351: 47–57.

661 [24] Galluzzi, L., Bugué, A., Kepp, O., Zitvogel, L., Kroemer, G., 2015.
662 Immunological effects of conventional chemotherapy and targeted anticancer
663 agents. *Cancer Cell*. 28: 690–714.

664 [25] Ishikawa, F., Yoshida, S., Saito, Y., Hijikata, A., Kitamura, H., Tanaka, S.,
665 Nakamura, R., Tanaka, T., Tomiyama, H., Saito, N., Fukata, M., Miyamoto, T.,
666 Lyons, B., Ohshima, K., Uchida, N., Taniguchi, S., Ohara, O., Akashi, K., Harada,
667 M., Shultz, L.D., 2007. Chemotherapy-resistant human AML stem cells home to
668 and engraft within the bone-marrow endosteal region. *Nat Biotechnol*. 25: 1315–
669 1321.

670 [26] Kalinski, P., Talmadge, J.E., 2017. Tumor immuno-environment in cancer
671 progression and therapy. *Adv Exp Med Biol*. 1036: 1–18.

672 [27] Keller, H.B., 1976. Numerical solution of two point boundary value problems.
673 Society for Industrial and Applied Mathematics, Philadelphia.

674 [28] Edelstein-Keshet, L., 1988. *Mathematical Models in Biology*. McGraw-Hill, New
675 York.

676 [29] Kirschner, D.E., Lenhart, S., Serbin, S., 1997. Optimal control of the
677 chemotherapy of HIV. *J Math Biol*. 35: 775–792.

- 678 [30] Kirschner, D.E., Linderman, J.J., 2009. Mathematical and computational
679 approaches can complement experimental studies of host-pathogen interactions.
680 *Cell Microbiol.* 11: 531–539.
- 681 [31] Krupar, R., Schreiber, C., Offermann, A., Lengerke, C., Sikora, A.G., Thorns,
682 C., Perner, S., 2018. Insilico analysis of anti-leukemia immune response and
683 immune evasion in acute myeloid leukemia. *Leuk Lymphoma.* 12: 1–4.
- 684 [32] Kuczynski, E.A., Sargent, D.J., Grothe, A., Kerbel, R.S., 2013. Drug rechallenge
685 and treatment beyond progression: implications for drug resistance. *Nat Rev Clin*
686 *Oncol.* 10: 571–587.
- 687 [33] Labianca, R., Sobrero, A., Isa, L., Cortesi, E., Barni, S., Nicoella, D., Aglietta,
688 M., Lonardi, S., Corsi, D., Turci, D., Beretta, G.D., Fornarini, G., Dapretto, E.,
689 Floriani, I., Zaniboni, A., 2011. Intermittent versus continuous chemotherapy in
690 advanced colorectal cancer: a randomised GISCAD trial. *Ann of Oncol.* 22: 1236–
691 1242.
- 692 [34] Lee, S., Chowell, G., 2017. Exploring optimal control strategies in seasonally
693 varying flu-like epidemics. *J Theor Biol.* 412: 36–47.
- 694 [35] Lee, J., Kim, J., Kwon, H., 2013. Optimal control of an influenza model with
695 seasonal forcing and age-dependent transmission rates. *J Theor Biol.* 317: 310–320.
- 696 [36] Lenhart, S., Workman, J.T., 2007. Optimal control applied to biological models.
697 Chapman & Hall/CRC, Taylor & Francis, London.
- 698 [37] Leung, C.Y., Weitz, J.J., 2017. Modeling the synergistic elimination of bacteria
699 by phage and the innate immune system. *J Theor Biol* 429: 241–252.
- 700 [38] Li, W., Todorov, E., 2004. Iterative linear quadratic regulator design for
701 nonlinear biological movement systems. *Proceedings of the 1st International*
702 *Conference on Informatics in Control, Automation and Robotics.* 1: 222–229.
- 703 [39] Lichtenegger, F.S., Krupka, C., Haubner, S., Köhnke, T., Subklewe, M., 2017.
704 Recent developments in immunotherapy of acute myeloid leukemia. *Journal of*
705 *Hematology and Oncology.* 10: 142.

- 706 [40] Liso, A., Castiglione, F., Cappuccio, A., Stracci, F., Schlenk, R.F., Amadori,
707 S., Thiede, C., Schnittger, S., Valk, P.J.M., Döhner, K., Martelli, M.F., Schaich,
708 M., Krauter, J., Ganser, A., Martelli, M.P., Bolli, N., Löwenberg, B., Haferlach,
709 T., Ehninger, G., Mandelli, F., Döhner, H., Michor, F., Falini, B., 2008. A one-
710 mutation mathematical model can explain the age incidence of acute myeloid
711 leukemia with mutated nucleophosmin (NPM1). *Haematologica*. 93: 1219–1226.
- 712 [41] MacLean, A.L., Celso, C.L., Stumpf, M.P.H, 2013. Population dynamics of
713 normal and leukaemia stem cells in the haematopoietic stem cell niche show
714 distinct regimes where leukaemia will be controlled. *J Royal Soc Interface*. 10:
715 20120968.
- 716 [42] Maclean, A.L., Filippi, S., Stumpf, M.P.H, 2014. The ecology in the
717 hematopoietic stem cell niche determines the clinical outcome in chronic myeloid
718 leukemia. *Proc Natl Acad Sci U.S.A.* 111: 3883–3888.
- 719 [43] Malik, T., Imran, M., Jayaraman, R., 2016. Optimal control with multiple
720 human papillomavirus vaccines. *J Theor Biol*. 393: 179–193.
- 721 [44] Masarova, L., Kanatarjian, H., GarciaMannero, G., Ravandi, F., Sharma, P.,
722 Daver, N., 2017. Harnessing the immune system against leukemia: monoclonal
723 antibodies and checkpoint strategies for AML. *Adv Exp Med Biol*. 995: 73–95.
- 724 [45] McGray, A.J.R., Bramson, J., 2017. Adaptive resistance to cancer
725 immunotherapy. *Adv Exp Med Biol*. 1036: 213–227.
- 726 [46] Mughal, T.I., Goldman, J.M., Mughal, S.T., 2010. Understanding leukaemias,
727 Lymphomas and Myelomas. Taylor & Francis, London.
- 728 [47] Murray, J.D., 2002. *Mathematical Biology I: An Introduction*, 3rd ed. Springer,
729 Heidelberg.
- 730 [48] Norton, M., 2014. *Modern Control Engineering*. Pergamon Unified Engineering
731 Series. Elsevier Science, Saint Louis.
- 732 [49] Ommen, H.B., Nvyold, C.G., Brændstrup, K., Andersen, B.L., Ommen, I.B.,
733 Hasle, H., Hokland, P., Østergaard, M., 2008. Relapse prediction in acute myeloid

734 leukaemia patients in complete remission using WT1 as a molecular marker:
735 development of a mathematical model to predict time from molecular to clinical
736 relapse and define optimal sampling intervals. *British Journal of Haematology*. 14:
737 782–791.

738 [50] Pontryagin, L.S., Boltyanskii, V.G., Gamkrelidze, R.V., Mischenko, E.F.,
739 1962. *The Mathematical Theory of Optimal Processes* [English translation].
740 Interscience, New York.

741 [51] Popat, U., Abraham, J., 2011. *Emerging Cancer Therapeutics: Leukaemia*.
742 Demos Medical Publishing, New York.

743 [52] Press, W.H., 2007. *Numerical recipes: the art of scientific computing*. Cambridge
744 University Press, New York.

745 [53] Priess, M.C., Conway, R., Choi, J., Popovich, J.M., Radcliffe, C., 2015. Solutions
746 to the inverse LQR problem with application to biological systems analysis. *IEEE*
747 *Transactions on Control Systems Technology*. 23: 770–777.

748 [54] Schrödl, K., Von Schilling, C., Tufman, A., Huber, R.M., Gamarra, F., 2015.
749 Response to chemotherapy, reexposure to crizotinib and treatment with a novel
750 ALK inhibitor in a patient with acquired crizotinib resistance. *Respiration*. 88:
751 262–264.

752 [55] Simpson, M.J., Landman, K.A., 2007. Analysis of split operator methods
753 applied to reactive transport with Monod kinetics. *Adv Water Resour*. 30: 2026–
754 2033.

755 [56] Simpson, M.J., 2009. Depth-averaging errors in reactive transport modeling.
756 *Water Resour Res*. 45: W02505.

757 [57] Sipkins, D.A., Wei, X., Wu, J.W., Runnels, J.M., Côté, D., Means, T.K., Luster,
758 A.D., Scadden, D.T., Lin, C.P., 2005. In vivo imaging of specialized bone marrow
759 endothelial microdomains for tumour engraftment. *Nature*. 435: 969–973.

760 [58] Tang, M., Gonen, M., Quintas-Cardama, A., Cortes, J., Kantarjian, H., Field,
761 C., Hughes, T.P., Branford, S., Michor, F., 2011. Dynamics of chronic myeloid

762 leukemia response to long-term targeted therapy reveal treatment effects on
763 leukemic stem cells. *Blood*. 118: 1622–1631.

764 [59] Thakur, M.D., Salangsang¹, F., Landman, A.S., Sellers, W.R., Pryer, N.K.,
765 Levesque, M.P., Dummer, R., McMahon, M., Stuart, D.D., 2013. Modelling
766 vemurafenib resistance in melanoma reveals a strategy to forestall drug resistance.
767 *Nature*. 494: 251–256.

768 [60] Warlick, E.D., Miller, J.S., 2011. Myelodysplastic syndromes: the role of the
769 immune system in pathogenesis. *Leuk Lymphoma*. 52: 2045–2049.

770 [61] Wiernik, P.H., Dutcher, J.P., Goldman, J.M., Kyle, R.A., 2013. Neoplastic
771 diseases of the blood. Springer, New York.

772 [62] Yakimov, A.S., 2016. Analytical solution methods for boundary value problems.
773 Academic Press, London.

774 [63] Zeidan, A.M., Mahmoud, D., Kucmin-bemelmans, I.T., Alleman, C.J., Hensen,
775 M., Skikne, B., Smith, B.D., 2016. Economic burden associated with acute myeloid
776 leukemia treatment. *Expert Rev Hematol*. 2016. 9: 79–89.